

HEARES 01313

Modelling the response of auditory midbrain neurons in the grassfrog to temporally structured monaural stimuli

Ivo H.M. van Stokkum

Department of Medical Physics and Biophysics, University of Nijmegen, The Netherlands

(Received 3 May 1989; accepted 28 August 1989)

In a previous paper [Van Stokkum and Gielen, *Hear. Res.* 41, 71–86, 1989] a model was presented to describe the processing of monaural stimuli by the auditory periphery of the grassfrog. The main components of this model were: a middle ear filter, transduction and tuning of the haircell, short-term adaptation, action potential (event) generation with refractory properties, and spatiotemporal integration of converging inputs. The model is now extended to model auditory midbrain neurons as third order neurons. The mechanisms that generate selectivity for temporal characteristics of sound are adaptation, coincidence detection of second order neurons, temporal integration of third order neurons, and most important, event generation of the first, second and third order model neurons. Variation of the parameters of the model successfully reproduces the range of response patterns which have been obtained from eighth nerve fibres, dorsal medullary nucleus neurons, and torus semicircularis neurons without inhibition. With a single set of parameters the output of the model in response to a set of spectrally and temporally structured stimuli qualitatively resembles the responses of a single neuron to all these stimuli. In this way the responses to the different stimuli are synthesized into a framework, which functionally describes the neuron.

Anuran; Auditory nerve; Dorsal medullary nucleus; Neural modelling; Temporal selectivity; Torus semicircularis

Introduction

Since the pioneering work of Potter (1965) the auditory midbrain of anurans has been the subject of much auditory research (for reviews see Fritzsche et al., 1988). Anurans use stereotyped, species-specific calls for intraspecific communication. In the grassfrog, *Rana temporaria*, these calls have a periodic pulsatile character (Fig. 1f). The pulses have a duration of 12 ms and a pulse repetition rate which, depending on temperature (Van Gelder et al., 1977; Walkowiak and Brzoska, 1982) varies between 20 and 40 Hz. The distinct temporal

character of the natural calls has led many investigators into a study of the coding of fine temporal characteristics of sound (for review see Walkowiak, 1988).

The auditory midbrain contains temporally selective neurons. In *Rana ridibunda* Bibikov (1971a, b) discovered that about half the midbrain units ceased to respond to an unmodulated tone within a few seconds, but fired continuously when this pure tone was replaced by a pulse train with a pulse duration of 8 ms and a PRR of 20 Hz. A further investigation of such neurons in *Rana temporaria* showed that at a constant PRR of 27 Hz the optimal pulse duration varied between 6 and 12 ms (Bibikov, 1980).

The selectivity for PRR has been investigated in the grassfrog by Schneider-Lowitz (1983) and Walkowiak (1984) in the NVIII, DMN, SON and TS. They studied the neuronal responses to trains of 10 ms pulses, with a train duration of 500 ms and a PRR varying between 5 and 100 Hz. Differing from their methods, the rate response to a

Correspondence to: Ivo H.M. van Stokkum, Dept. of Medical Physics and Biophysics, University of Nijmegen, P.O. Box 9101, 6525 EZ Nijmegen, The Netherlands.

Abbreviations: AMF, amplitude modulation frequency; DMN, dorsal medullary nucleus; EPSP, excitatory postsynaptic potential; NVIII, eighth nerve; PRR, pulse repetition rate; SNR, signal-to-noise ratio; SON, superior olivary nucleus; SPL, sound pressure level; TS, torus semicircularis.

pulse train was divided by the number of pulses in a study by Van Stokkum (1989: p. 14). The resulting number of spikes per stimulus pulse as function of PRR was taken as a measure to classify the responses. A response was classified as selective if the response above or below a certain cut-off PRR was less than 50% of the maximum response. In the lowest three stations of the auditory pathway, the NVIII, DMN and SON, two response types are present: non-selective and low-pass. The percentage of low-pass responses increases from about 20% in the NVIII to about 75% in DMN and SON. The cut-off PRRs of these low-pass responses were between 10 and 60 Hz, a range which encompasses the PRRs of natural calls. In the TS 12% of the units showed a non-selective response, and 56% showed a low-pass response. Furthermore three new response types emerged in the TS, 6% of the neurons responded only to the highest PRRs (high-pass), 8% responded exclusively to a small range of PRRs (band-pass) and 18% showed the opposite behavior (band-suppression or bimodal).

With another class of stimuli, amplitude modulated sounds, both the rate aspect of the response and the synchronization aspect have been studied in the NVIII and TS (Rose and Capranica, 1983, 1984, 1985; Epping and Eggermont, 1986b). With respect to rate the responses were classified into the above mentioned five categories. The synchronization index showed a non-selective or low-pass behaviour as function of AMF. NVIII fibres synchronized their firings to the envelope of the amplitude modulator. This synchronization capability was retained for AMFs above 100 Hz (Rose and Capranica, 1985). In contrast, the firings of 38% of the TS units were not significantly synchronized to the envelope (Epping and Eggermont, 1986b). In the other TS units synchronization to the envelope was a low-pass function of AMF, with lower cut-off AMFs than found in the NVIII (Rose and Capranica, 1985).

An explanation for these different types of responses to temporally structured stimuli can be found in the integrative properties of neurons. The cable properties of neurons, especially of their dendrites, cause temporal integration of inputs (Rall, 1977). NVIII fibres have integration times smaller than 1 ms (Dunia and Narins, 1989) allow-

ing them to synchronize their firings to stimulus envelopes with AMFs greater than 100 Hz. Likewise, DMN neurons have integration times of 1–5 ms (Bibikov and Kalinkina, 1983), which still enables them to pass on the synchrony code. But in the TS Bibikov (1974, 1977, 1978) found integration times ranging from 1 to 100 ms. These integration times were determined from the time course of the probability of spike generation in response to a tone just above threshold (see also Van Stokkum, 1989, p. 12–13). TS units with long integration times lose their synchronization capability, but may develop selectivity for PRR by temporal integration of consecutive inputs. The hypothesis that temporal integration is responsible for the new types of temporal selectivity in the TS will be tested quantitatively with help of a model. Another hypothesis is that local circuits in the TS are responsible for the development of temporal selectivity. This second hypothesis will be investigated by recording simultaneously from pairs of single units, and looking for the presence of neural interaction.

In a previous paper (Van Stokkum and Gielen, 1989) a model was developed for NVIII and DMN neurons. This model for first and second order auditory neurons is now extended to produce the responses of third order neurons. In *Ranidae* the main ascending auditory inputs to the TS come from the ipsilateral SON and from the ipsi- and contralateral DMN (Wilczynsky, 1988). In view of this TS neurons can be considered as third or fourth order auditory neurons. The known temporal selectivities of SON neurons deviate only slightly from those of DMN neurons. This justifies the simplification to model TS neurons as third order neurons, thereby reducing the number of degrees of freedom for the modeller. Care was taken to keep the characteristics of first and second order model neurons in line with data from the literature and with those used in the previous model (Van Stokkum and Gielen, 1989).

To characterize TS neurons a broad ensemble of stimuli was used to explore the selectivity for carrier frequency, PRR, AMF and pulse shape. The main goal of this paper was to describe the selectivities of some typical TS neurons, and to compare their responses to a set of stimuli with the responses of a model neuron. Matching the

responses of the model neuron to the neurophysiological data enabled us to find a reliable set of parameters for the model. Similarities between the selectivities of the real and model neuron indicate the plausibility of the model for the temporal processing in the TS. It will be shown that spatio-temporal integration of second order inputs reproduces the new types of temporal selectivity found in the TS.

Methods

Animal preparation and recording procedure

Adult grassfrogs (*Rana temporaria* L.) from Ireland were anaesthetized with a 0.05% solution of MS-222. A hole was drilled into the parietal bones above the midbrain, leaving the dura intact. The animal was allowed to recover overnight. The next day it was immobilized with an intralymphatic injection of Buscopan (0.12 mg per gram bodyweight). A local anaesthetic, Xylocaine 2%, was applied to the wound margins. The animal was placed in a sound attenuated room (IAC type 1202A) onto a damped vibration-isolated frame. Temperature was maintained around 15°C and the skin was kept moist to aid cutaneous respiration. The animal's condition was monitored with help of ECG recording (Epping and Eggermont, 1987) and by examination of the blood flow in superficial vessels below the dura. The preparation was usually kept intact for two days.

Ultrafine or tapered tungsten microelectrodes (Micro Probe Inc.), coated with Parylene-c, having a 5–25 µm exposed tip and a 1 kHz impedance of 1–5 MΩ were used for extracellular recording. Using hydraulic microdrives two independent electrodes, tip distance on the roof of the midbrain between 100 and 400 µm, were lowered into the TS and separable few-unit recordings were obtained with help of a spike separation procedure (Epping and Eggermont, 1987). Waveform features and spike epochs were stored on a PDP 11/34 with a resolution of 40 µs, and analyzed off-line with a PDP 11/44 and a VAX 11/785.

Acoustic stimulus presentation and response analysis

The acoustic stimuli were generated by a programmable stimulus generator, as described by

Epping and Eggermont (1985). The stimuli were presented to the animal by two electrodynamic microphones (Sennheiser MD211N) coupled to the tympanic membrane using a closed sound system. The frog's mouth was kept open during the experiment, in order to decouple both ears (Vlaming et al., 1984). The sound pressure level was measured in situ with a half inch condenser microphone (Brüel and Kjaer 4143) connected to the coupler. The frequency response of the system was flat within 5 dB for frequencies between 100 and 3000 Hz, a sufficient range for studying the auditory system of the grassfrog (Brzoska et al., 1977). The amplitude characteristics of the left and right coupler were equal within 2 dB for the range of interest. The stimuli were usually presented contralaterally with respect to the recording site, at sound pressure levels of 70 to 100 dB peak. These sound pressure levels are sufficient to evoke behavioural responses (Walkowiak and Brzoska, 1982; Brzoska, 1984).

The following stimulus ensembles have been used:

(1) *Tonepips (Fig. 1a)*. To study spectral selectivity tonepips of 46 ms duration, modulated with a gamma envelope (Aertsen and Johannesma, 1980), were presented once per second. The carrier frequency was chosen pseudorandomly from 45 logarithmically equidistant values between 0.1 and 5 kHz. Also a rectangular envelope was used for the tonepips, with a duration of 100 ms and rise and fall times of 5 ms. To study two-tone suppression a second tonepip at the neuron's best frequency, attenuated by 0, 10 or 20 dB with respect to the tonepip stimulus, was presented simultaneously.

(2) *Pulse shape variations (Fig. 1b)*. To study the effect of pulse shape a sequence consisting of a click, a pulse from the mating call, tonepips, gammatones, and if appropriate also their time-reversed versions, was used. The tonepips had 1 ms rise and fall times and durations of 5, 10, 20 and 50 ms. The gammatones had rise and fall times of, respectively, 20% and 80% of 10, 20 and 50 ms. The peak amplitude of the click was ten times that of the other pulse shapes. The neuron's best frequency was chosen as carrier frequency for the

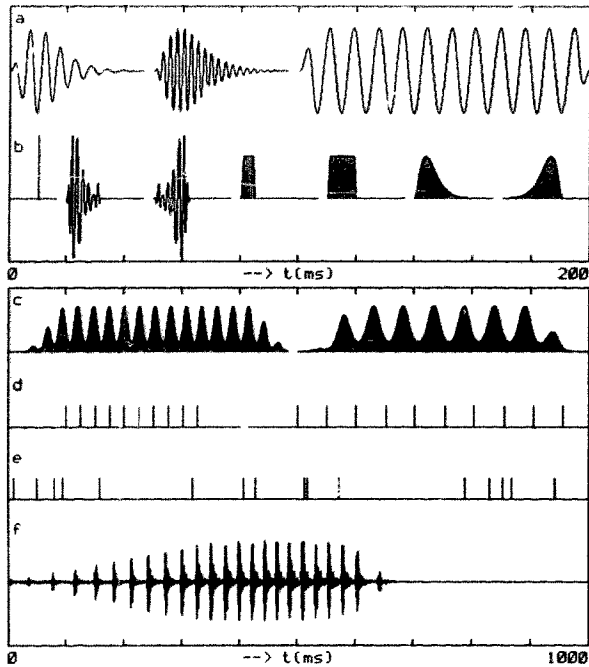


Fig. 1. Stimulus waveforms and envelopes. (a) two gammatones of 46 ms duration and a 100 ms tonepip; (b) click, normal and time-reversed pulse from the mating call, envelopes of tonepips of 5 and 10 ms duration, normal and time-reversed gammatones of 20 ms duration; (c) envelope of two AM tonebursts; (d) two periodic click trains; (e) segment from random click ensemble; (f) mating call, recorded at 15°C.

tonepips and gammatones. Onset interval of the pulse shapes was 1 s.

(3) *Sinusoidally amplitude modulated tone bursts* (Fig. 1c). Tone bursts of 500 ms duration with 100 ms overall rise and fall times were presented every 3 s. The neuron's best frequency was chosen as carrier. The modulation depth was 16 dB, corresponding to 84%. The AMFs were varied pseudorandomly between 7.8 and 250 Hz. In addition an unmodulated tone burst was presented (Epping and Eggermont, 1986b).

(4) *Spectrotemporal stimulus*. Amplitude modulated sound bursts with different carriers were used to study the interdependency of spectral and temporal selectivity. Onset interval of the 500 ms duration sound burst was 2 s. One spectrotemporal stimulus consisted of combinations of four

carriers with three modulators (100% modulation depth), another stimulus contained combinations of six carriers with five modulators (84% modulation depth, Fig. 1c).

(5) *Periodic click trains* (Fig. 1d). Trains of 10 equidistantly spaced clicks, with onset intervals of 3 s. The interclick intervals of the trains were varied pseudorandomly between 128 and 4 ms, corresponding with logarithmically equidistant PRRs of 7.8 to 250 Hz. The duration of the condensation click was 0.7 ms, and its amplitude spectrum was flat within 5 dB for the range of interest (Epping and Eggermont, 1986a).

(6) *Random clicks* (Fig. 1e). Stimulus ensemble consisting of clicks with an average rate of 16/s. The interclick intervals are drawn independently from a negative exponential distribution with a minimum interval of 1 ms. The interval distribution corresponds to a Poisson process with a dead-time of 1 ms (Epping and Eggermont, 1986a).

(7) *Mating call ensemble*. The basic sequence consisted of 10 s silence, followed by three original mating calls (Fig. 1f). After this the envelope of the original mating call served as amplitude modulator for carrier frequencies of 201, 557, 1067 and 1542 Hz. Then, while keeping the number of pulses constant, the interpulse intervals of the original mating call were multiplied by 0.5, 1, 2 and 4, corresponding with PRRs of 72, 36, 18 and 9 Hz. Finally the original mating call was presented again followed by its time-reversed version. Intervals between the calls were about 2.5 s. This basic sequence, which had a duration of 50 s, was first presented in silence. Thereafter a pink noise background, whose amplitude was increased stepwise, was added to the basic sequence. The peak ratios between vocalizations and noise (SNR) were consecutively 6, 0 and -6 dB. After the basic sequence with the highest noise level a 50 s period of silence was added (Eggermont and Epping, 1986).

To check the reproducibility of the responses and to collect adequate data all stimuli were repeated at least three times. The response to the random clicks was analyzed by crosscorrelating the stimulus clicks (z_1) with the neural response

(z_2), resulting in a crosscoincidence histogram (CCH). The formula for bin m of the CCH reads:

$$CCH_{12}(m) = \frac{1}{T\Delta} \int_0^T dt \int_{(m-\frac{1}{2})\Delta}^{(m+\frac{1}{2})\Delta} d\tau z_1(t) z_2(t+\tau) \quad (1)$$

Here $z_i(t) = \sum_{j=1}^{N_i} \delta(t - t_{i,j})$ represents the events at times $t_{i,j}$ of point process z_i , T is the duration of the experiment and Δ is the binwidth of the crosscoincidence histogram.

The responses to the other stimuli are presented in the figures as reordered eventdisplays along with spike rate histograms. Thereby the actual response is reordered systematically according to a stimulus parameter. In this paper spike rate is defined as the average number of action potentials per stimulus presentation.

The presence of neural interaction was investigated by crosscorrelation of simultaneously recorded spike trains (Epping and Eggermont, 1987; Melssen and Epping, 1987). Neural synchrony resulted in a peak or trough in the simultaneous crosscoincidence histogram (Eq. 1, with z_1 and z_2 the responses of the two neurons). The contribution of a common stimulus influence to this synchrony was estimated by the nonsimultaneous crosscoincidence histogram (NCH), also called shift predictor (Perkel et al., 1967). The nonsimultaneous crosscoincidence histogram results from crosscorrelation of one unit's spike train with the spike train of the other unit shifted circularly over the length L of a stimulus sequence (Eq. 2). Hereby it was verified that the responses of the neurons were periodically stationary, i.e. that the response probability remained identical for subsequent stimulus sequences.

$$NCH_{12}(m) = CCH_{12}\left(m + \frac{L}{\Delta}\right) \quad (2)$$

A difference between the simultaneous and nonsimultaneous crosscoincidence histogram indicates that the neural synchrony is not merely caused by stimulus influences, but that neural interaction also contributes.

The model

As a starting point a simplified version of the model for the peripheral auditory system (Van Stokkum and Gielen, 1989) is taken. The model's components are shortly described below and are shown in Fig. 2. A cascade consisting of a linear middle ear filter (Fig. 2A, impulse response in Eq. 3), a linear band-pass filter (Fig. 2B, impulse response in Eq. 4), and a static nonlinearity (Fig. 2C, Eq. 5) produces a haircell potential u . The middle ear filter, which was derived from Aertsen et al. (1986), is described by the resonance frequency ω_1 and decay rate γ :

$$h(t) = 2\gamma e^{-\gamma t} \sin(\omega_1 t) \Theta(t) \quad (3)$$

with $\Theta(t) = 1$ if $t > 0$, and $\Theta(t) = 0$ if $t \leq 0$. The band-pass filter impulse response $f_i(t)$ is characterized by a centre frequency ω_i and by a time constant β_i which determines the sharpness of the filter.

$$f_i(t) = 2\beta_i^{-2} t e^{-t/\beta_i} \sin(\omega_i t) \Theta(t) \quad (4)$$

Parameter r^0 of the mechano-electrical transduction non-linearity (Eq. 5, Fig. 2C) is related to the half-saturation sound pressure level (Crawford and Fettiplace, 1981).

$$u(r) = \frac{r}{r + r^0} \Theta(r) \quad (5)$$

The haircell potential u provides the input to an adaptation component which was adopted from Eggermont (1985), and which is described by an inactivation rate λ and a recovery rate μ (see Van Stokkum and Gielen, 1989):

$$v = (u + b) \Theta(u + b) \quad (6)$$

$$\frac{db}{dt} = -\lambda v - \mu b \quad (7)$$

The differential equation for b corresponds to that describing a first-order low-pass filter. Note that omission of the rectifier (Fig. 2F) would leave us with a high-pass filter. Low-pass filtering by the dendrites of the NVIII neuron (Fig. 2G, impulse

response in Eq. 8) produces the generator potential w of the first order model neuron.

$$I(t) = \omega_2^- \omega_2^t \Theta(t) \tag{8}$$

Action potentials (events) are generated stochastically with help of a generator function $g(w)$, known in point process literature (e.g. Cox and Isham, 1980) as the intensity function. The probability of event generation in a bin with width Δt is (see Van Stokkum and Gielen, 1989):

$$P[\Delta N(t) = 1] = 1 - e^{-g(w)\Delta t} \tag{9}$$

Here $N(t)$ is the counting process, which represents the number of events up to time t , and $\Delta N(t) = N(t + \Delta t) - N(t)$. The argument of the generator function depends in two ways on the events generated in the past. Firstly, after an event has been generated the probability per unit of time to generate an event, $g(w)$, is zero for an absolute refractory period τ_{abs} . Secondly, to model relative refractoriness a negative feedback is supplied to the event generator. This feedback is given by the impulse response $c(t)$, which starts after the end of τ_{abs} :

$$c(t) = -Re^{-(t-\tau_{abs}/\tau_R)}\Theta(t - \tau_{abs}) \tag{10}$$

The refractory mechanism is illustrated in Figs. 2E and 2I, with $\tau_{abs} = 1$ ms and $\tau_R = 2$ ms. When τ_R is much larger than τ_{abs} the negative feedback produces adaptation of the model neuron (see also Bibikov and Ivanitskii, 1985). For the generator function $g(w)$ a half-linear function is chosen:

$$g(w) = \nu(w - m)\Theta(w - m) \tag{11}$$

When the generator potential w is less than m , the threshold parameter, $g(w)$ is zero. Parameter ν determines the slope of $g(w)$. In Figs. 2H, K the probability of event generation according to Eqs. 9 and 11 is drawn for two different values of ν .

Spatiotemporal integration of inputs

It is assumed that lower order neurons converge upon a higher order neuron. This convergence of inputs is modelled as a linear summation of the input point processes, which are then low-

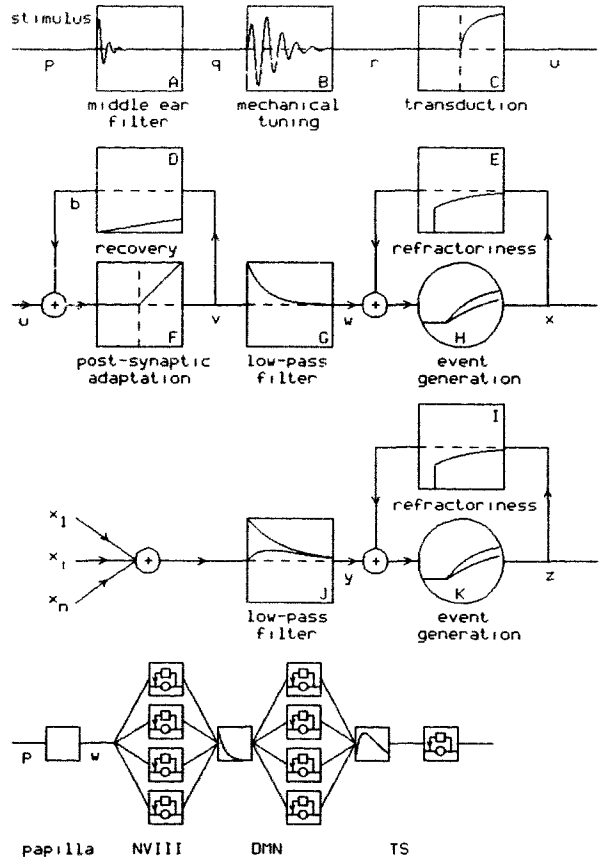


Fig. 2. Model for the processing of sound by the papilla, NVIII, DMN and TS of the grassfrog. The stimulus waveform is band-pass filtered by the middle ear (Fig. 2A), and filtered and transduced into a haircell potential (Figs. 2B, C). The synapse between the haircell and the dendrite of the NVIII fibre comprises of a short-term adaptation mechanism (Figs. 2D, F) and a low-pass filter (Fig. 2G). From the generator potential w of the NVIII fibre action potentials are generated (Fig. 2H), which form the point process x . Absolute and relative refractory mechanisms are incorporated in the negative feedback loop (Fig. 2E). Outputs from lower order neurons ($x_1, \dots, x_i, \dots, x_n$) converge upon a higher order neuron, where they add linearly and are convoluted with an EPSP shape (Fig. 2J). From the generator potential y of the higher order neuron action potentials are generated in the same way as explained above. In Figs. 2A, B, D, E, G, I and J impulse responses are drawn on a timebase of 5 ms. Figs. 2C and F represent the instantaneous nonlinearities of, respectively, Eqs. 5 and 6. Figs. 2H, K show probabilities of event generation (Eqs. 9, 11) as function of the generator potentials w, y . The lower flow diagram symbolizes the connections used in the simulations of this paper. The generator potential w is used to generate events in four NVIII units. Four DMN units receive input from these four NVIII units. Finally the four DMN units converge upon the third order model neuron, which represents a TS neuron. One EPSP shape is used between NVIII and DMN, and another EPSP shape is used between DMN and TS. Further explanation in text.

pass filtered to arrive at compound EPSPs. In formula (Johannesma and Van den Boogaard, 1985):

$$y(t) = \sum_{i=1}^n \int ds e_i(s) x_i(t-s) \quad (12)$$

with

$$e_i(t) = W e^{-t/\tau_d} (1 - e^{-t/\tau_u}) \Theta(t) \quad (13)$$

Here $x_i(t) = \sum_{j=1}^{N_i} \delta(t - t_{ij})$ represents the events at times $t_{i,j}$ of lower order neuron i . In Fig. 2J different EPSP shapes $e_i(t)$ are drawn. In the lower part of Fig. 2 a schematic diagram for a third order neuron is illustrated. The generator potential w provides input to four NVIII neurons, which differ in threshold and absolute refractory period. Spatiotemporal integration of these four NVIII inputs produces a generator potential y for four DMN neurons with different thresholds. Finally spatiotemporal integration of these four DMN inputs produces a generator potential y for a TS neuron. Each model neuron box consists of an event generator and a negative feedback provided by the refractory mechanisms.

Implementation of the model

The model was programmed in Fortran 77 on a VAX 11/785 computer. The seven stimuli were sampled and provided the input to the model. The sample interval was 0.1 ms for stimuli 1-3, and 0.2 ms for stimuli 4-7. The number of stimulus presentations usually differs between real and model neuron. Because of limited computer capacity the duration of the mating call stimulus (250 s) was shortened to 120 s by reducing the intervals between the calls to 1.4 s. The time-constant for recovery from adaptation (μ^{-1}) was limited to 1 s, in order to minimize forward masking of consecutive responses to the mating call variations.

A summary of the parameters used in the simulations of this paper is given in Table I. The degrees of freedom are: the tuning characteristics, the stimulus amplitude relative to r^0 , the degree of spatiotemporal integration (EPSP shape) and, most important, the parameters which determine the event generation and refractory properties.

Outputs of the model are the generator potentials w and y of, respectively, the first and higher order neuron, and the time-series x and z , which mimic the occurrences of action potentials in, respectively, a first or higher order neuron. The generator potentials help us to understand the

TABLE I
MODEL PARAMETERS

Parameters	Eq.	Related to	Value
γ, ω_1	3	middle ear filter	$1.297 (\text{ms})^{-1}, 2\pi \cdot 0.876 \text{ kHz}^a$
ω_1, β_i	4	tuning characteristics	variable, 1 ms
r^0	5	transduction saturation	1
λ^{-1}, μ^{-1}	7	short-term adaptation	10 ms, 1000 ms
ω_2	8	dendritic low-pass filter	$1 (\text{ms})^{-1}^b$
$\tau_{\text{abs}}, R, \tau_R$	10	refractory properties	NVIII: 3-6 ms, 2, 1 ms DMN: 6 ms, 0.015, 400 ms TS: variable
m, ν	11	event generation	NVIII: $0.0001-0.001, 100 (\text{ms})^{-1}$ DMN: variable, $40 (\text{ms})^{-1}$ TS: variable
n	12	amount of convergence	4
W	13	EPSP height	0.2
τ_d, τ_u	13	EPSP shape	NVIII \rightarrow DMN: variable, 0 ms DMN \rightarrow TS: variable NVIII \rightarrow DMN: 2 ms DMN \rightarrow TS: variable
		time delay	

^a Derived from Aertsen et al. (1986), p. 21, 25.

^b Crawford and Fettiplace (1980), p. 91.

action of the several nonlinearities incorporated in the model. The time-series z , or averages thereof in the form of histograms, can directly be compared to experimental data obtained in higher order neurons.

Results

Data base

Recordings were made from 161 auditory mid-brain neurons in 30 grassfrogs. Stimuli 1, 2 and 3 were presented to almost all units. At least five different stimuli were presented to 54 units. Fifteen units were fully characterized. A full characterization requires the presentation of all seven stimulus ensembles and comprises investigation of the different kinds of selectivities at several intensities.

In Table II a summary of the rate responses to the click train, pulse shape and mating call stimuli is given. The different response types as determined with the click trains have already been explained in the Introduction. A response was classified as selective if the response decreased by at least 50% relative to the maximum response. The PRR evoking a 50% response was termed the cut-off PRR.

TABLE II
SUMMARY OF RATE RESPONSES TO PULSE SHAPE VARIATIONS (HORIZONTAL) AND PERIODIC CLICK TRAINS (VERTICAL)

	Integration effect		no response	total
	no	yes		
Non-selective	9 (---)			9
Low-pass	10 (-)			10
High-pass	2	9 (+)		11
Band-pass		8 (+-)	5 (+++)	13
Bimodal	1	1 (+)		2
No response	3	6 (++)	2 (+)	11
Total	25	24	7	56

When the response was restricted to pulse shapes exceeding a minimum duration, a temporal integration effect was considered to be present. Fourteen units with a particular rate response type with respect to PRR in the mating call ensemble are indicated between parentheses: +: high-pass, -: non-selective. Further explanation in text.

Some units responded only to pulse shapes exceeding a minimum duration, an example is shown in Figs. 5a, b. Usually this was accompanied by a larger response to the time-reversed versus the normal pulse shapes, see e.g. the response to the time-reversed gammatones of 20 and 50 ms in Fig. 5b. This type of response to pulse shapes is interpreted as evidence for the presence of temporal integration. Twenty-five units did not, and twenty-four units did show a temporal integration effect. Out of the neurons without a visible integration effect three showed a preference for pulse shapes of short duration and one for short rise times.

Eight of the 11 units which did not respond to the click trains were strongly inhibited by frequencies around 600 Hz. The two units which showed a bimodal response both showed an inhibition followed by excitation response type as determined with the random clicks (type III of Epping and Eggermont, 1986a). The distribution of the response types with the click trains agreed with the findings of Epping and Eggermont (1986a). Neurons which showed clear signs of integration effects (column two in Table II) showed a high-pass, band-pass or no response to the click trains. However, nearly all units without visible integration effects (column one) showed a non-selective or low-pass response to the click trains. Units which did not respond to the pulse shapes (column three) showed a band-pass or no response to the click trains. The neurons which preferred the higher PRR variations of the mating call (indicated by +) are all contained in columns two and three. Because only four PRR-variations of the mating call were tested no detailed classification was made.

Rows one and two have been lumped and also rows three, four and five in order to perform a χ^2 statistical test. The selectivity for pulse shapes and for click trains were not independent ($\chi^2 = 36.5$, $df = 4$, $P < 0.05\%$). This strengthens the hypothesis that temporal integration effects are responsible for the band-pass and high-pass response characteristics, which appear for the first time in the TS.

About 40% of the data were obtained while simultaneously recording from two or three units. Table III summarizes the inferences made from

TABLE III
SUMMARY OF UNIT PAIR ANALYSIS

	Recorded on		
	1 electrode	2 electrodes	Total
No synchrony	1	2	3
Synchrony	11	18	29
Common input	3	2	5

crosscorrelations of 32 pairs of units. The great majority of these, 29 pairs, showed signs of neural synchrony, visible as a peak or trough in the simultaneous crosscoincidence histogram. A clear difference between the simultaneous and non-simultaneous crosscoincidence histogram was seen in only five of these 29 pairs. Most probably the differences have to be ascribed to neural common input. No clear differences were observed between unit pair recordings made from one or two electrodes. Thus in agreement with a larger study by Epping and Eggermont (1987) neural interaction seems to play a minor role in the auditory mid-brain of immobilized anurans. Therefore the hypothesis that local circuits are responsible for temporal selectivity was abandoned (however, see Discussion). In the following a model will be elaborated which predicts responses of TS units from convergent input from lower order neurons, disregarding interactions between TS units.

Modelling two typical TS units

It will be shown how the model produces a high-pass response to the click train stimulus by means of temporal integration. Then the complex of selectivities found for a TS unit showing temporal integration and a high-pass response to the click trains will be compared with the model neuron's selectivities.

In Fig. 3 the response of the first and second order model neuron to the click trains is shown. The second order model neuron receives four inputs (Fig. 2). The absolute refractory periods of the NVIII inputs vary linearly between 3 and 6 ms, and their thresholds vary linearly between 0.001 and 0.0001. The NVIII input with the highest threshold and the longest τ_{abs} is illustrated in Figs. 3a, b. The first and second order neuron

both show rate responses of a low-pass type with a cut-off PRR of 200 Hz (Figs. 3b, d). This is caused mainly by the absolute refractory period of 6 ms which interferes with the highest PRRs. Note that there is a one to one correspondence between stimulus and response up to a PRR of 100 Hz.

As a next step an EPSP (Eq. 13) with a fall time-constant τ_d of 30 ms and a rise time of 24 ms ($\tau_u = 60$ ms) is chosen to model the temporal integration. These time constants were chosen in order to fit the response of neuron 322, 3, 0 (Fig. 5). In Fig. 4a the spatiotemporal integration performed by the third order model neuron is visible in the generator potential, averaged over the en-

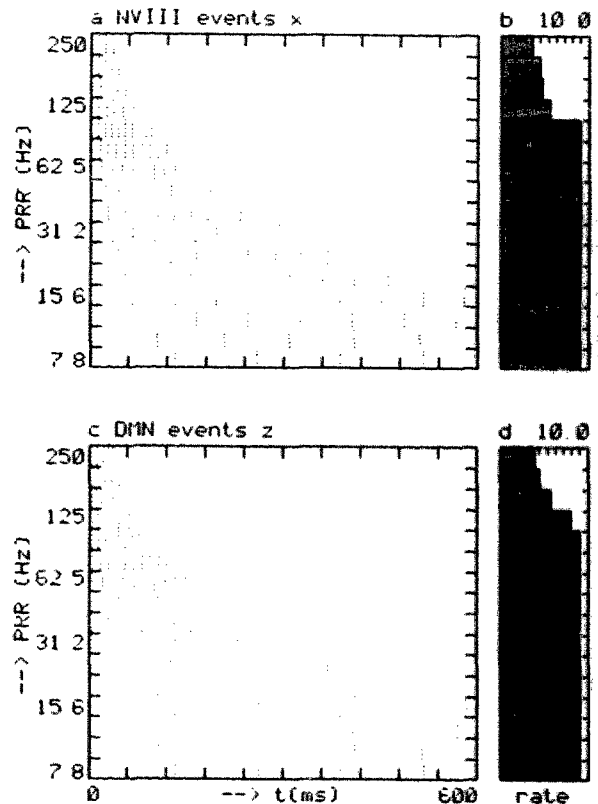


Fig. 3. Recorded event displays together with rate histograms of responses of first and second order model neurons to the periodic click trains. Stimulus intensity: 22 dB relative to r^0 . Model parameters: tuning: centre frequency 0.4 Hz; first order event generation: m 0.001, τ_{abs} 6 ms. The second order unit receives input from four units as in (a), with m varying linearly between 0.0001 and 0.001 and τ_{abs} varying linearly between 3 and 6 ms. Further model parameters: EPSP shape: τ_d 3 ms; second order event generation: m 0.33. A delay of 2 ms was incorporated.

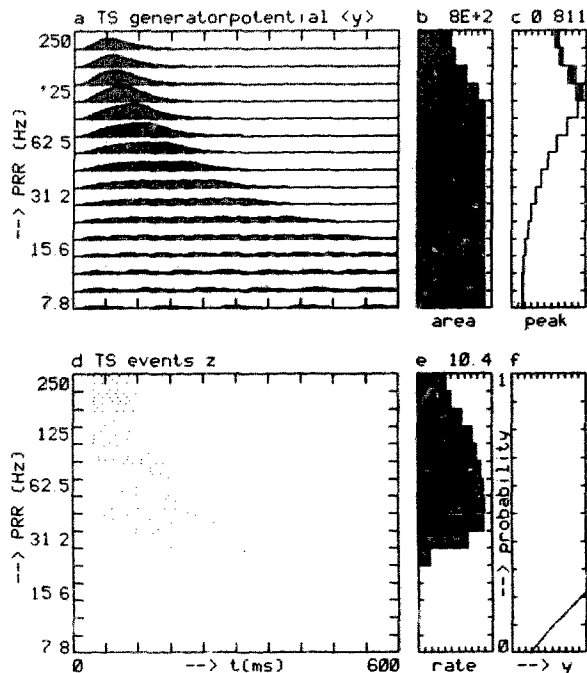


Fig. 4. Simulation of a TS neuron, which receives input from four DMN neurons as in Figs. 3c, d. Outputs y , the generator potential, and z , the events, as a function of PRR. The time-course of the ensemble averaged generator potential $\langle y(t) \rangle$ (a), its area (b) and the average and standard deviation of the peak of $y(t)$ (c) are depicted. Inputs are four units, with m varying linearly between 0.27 and 0.33. The m -value of 0.33 was used in Figs. 3c, d. EPSP parameters: τ_r 60 ms, τ_d 30 ms. Parameters for the TS event generation: ν 2 (ms) $^{-1}$, m 0.21. Refractory parameters: τ_{obs} 10 ms, R 0.6, τ_R 2 ms. A delay of 10 ms was incorporated in order to fit the latency.

semble of five stimulus presentations. The negative feedback provided by the refractory mechanisms has been excluded from Figs. 4a–c. Fig. 4b shows the average area of the generator potential as a function of PRR. The solid line in Fig. 4c corresponds with the average peak of the generator potential, and the deviations from the solid line correspond with the standard deviation of this peak. A high-pass character is clearly visible in Fig. 4c. The probability of event generation function (Eqs. 9, 11) in Fig. 4f, which for comparison is drawn to the scale of Fig. 4c, is now used to generate the response shown in Figs. 4d and 4e. Because of the high threshold a single click produces no response, and temporal integration is necessary to reach threshold. Note that in contrast

to Fig. 3 the synchronization to the individual stimulus clicks is lost.

The responses of unit 322,3,0 and of the model neuron to six stimuli are compared in Figs. 5 and 6. Because unit 322,3,0 responds to carrier frequencies up to 1.0 kHz (Fig. 5e) it receives excitatory input originating from the amphibian papilla. This is modelled with a band-pass filter (Eq. 2) tuned to 0.4 kHz, the unit's best frequency. Threshold of this unit was 50 dB peak SPL. At intensities of 70 and 90 dB the unit showed practically no response to pulse shapes with a duration shorter than 20 ms (Figs. 5a, b). This is very well reproduced by the model neuron (Figs. 6a, b). The responses to the click trains, Figs. 5c and 6c, show a high-pass character and a decline of latency with increasing PRR. Quantitatively however, the model neuron's response is stronger for PRRs between 40 and 100 Hz. The crosscoincidence histograms between the clicks and the events (Figs. 5d and 6d) both show a broad peak, whose width is somewhat smaller for the model neuron. The greatest deviation between data and simulation is found with the spectrotemporal stimulus (Figs. 5e and 6e). Unit 322,3,0 responds well to the onset of unmodulated tones, and this onset response is followed by a rebound in case of the 0.5 kHz carrier. This pause response pattern might be caused by inhibition, which was not included in the model. Furthermore the rate response of Fig. 5e shows a high-pass character with respect to AMF. This is modelled with a modest degree of coincidence detection on the DMN level. In a previous paper (Van Stokkum and Gielen, 1989) it was demonstrated that part of the DMN units respond selectively to fast intensity changes. These fast intensity changes synchronize the NVIII inputs, and convergence of these inputs upon a DMN unit, using a short integration time, produces a peaked generator potential. In contrast, an unmodulated tone produces a flatter generator potential, because the input firings will gradually become distributed in time, due to their refractory properties. The thresholds of the DMN units of this model produced a modest high-pass response with respect to AMF (not shown). This modest high-pass response is preserved on the TS level (Fig. 6e). Finally in Figs. 5f and 6f the response to the mating call ensemble is depicted. Without

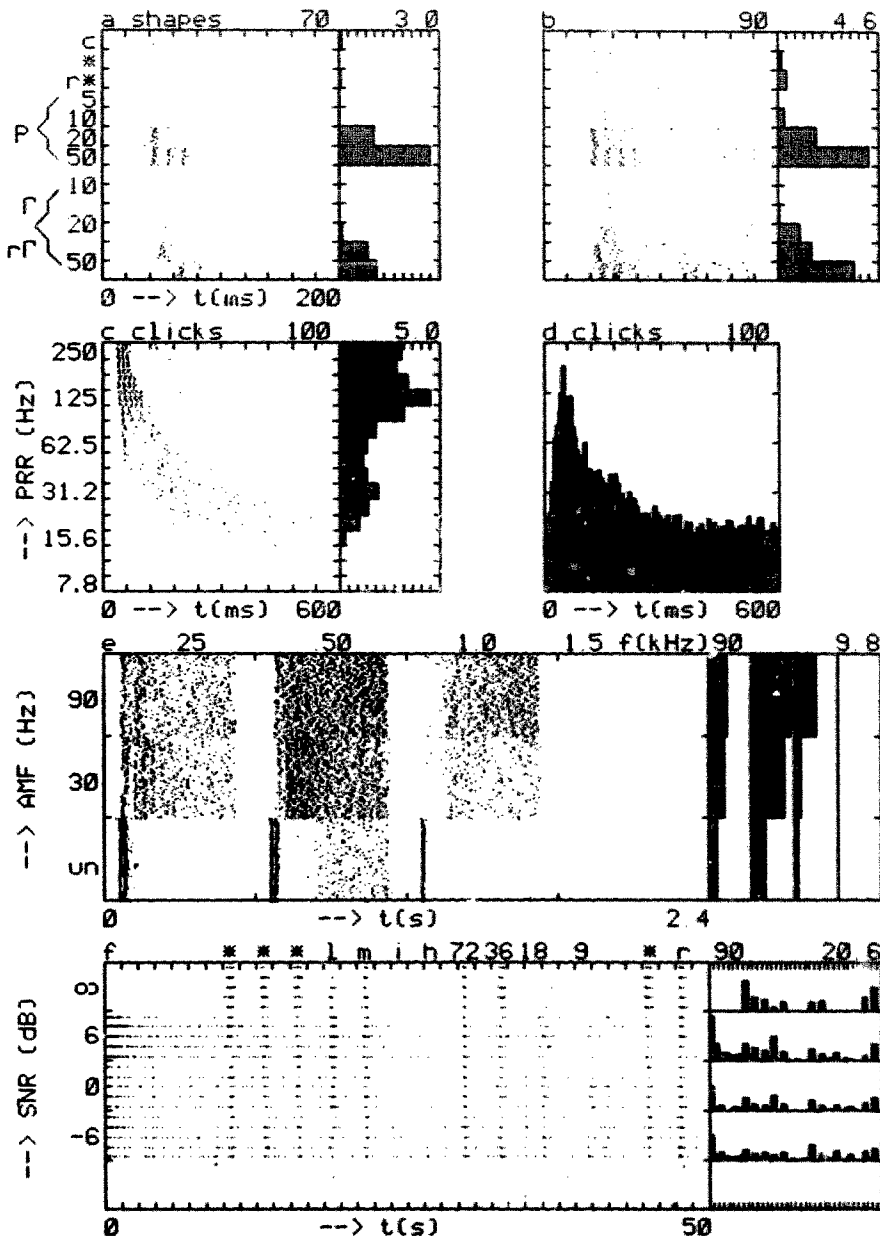


Fig. 5. Reordered eventdisplays together with rate histograms of responses of TS unit 322.3.0 to six different stimuli. At the left the stimulus parameter variation is indicated. All stimuli were presented contralaterally. The intensities, in dB peak SPL, are indicated above each eventdisplay. Carrier frequency in Figs. a and b was 0.5 kHz. Above each rate histogram the maximum value is written. Note the different timebases, which are indicated under the eventdisplays. In Fig. d the crosscoincidence histogram between the random click stimulus and the events is drawn. The different pulse shapes in Figs. a and b were: click (c), pulse from the mating call (*), tonepip (p), gammatone (Γ), and time-reversed versions (r^* and $r\Gamma$). The durations (in ms) of the tonepips and of the gammatones are indicated. The equidistant click trains of Fig. c consisted of 10 clicks with PRR varying between 7.8 and 250 Hz. With the spectrotemporal stimulus (Fig. e) carrier frequency varies horizontally, whereas AMF varies vertically. In addition to tonebursts with AMFs of 30 and 90 Hz an unmodulated toneburst (un) was presented. The mating call ensemble (Fig. f) was first presented in silence (SNR ∞). Next a stepwise pink noise background was added (SNR decreasing from 6 to -6 dB). Further explanation in text.

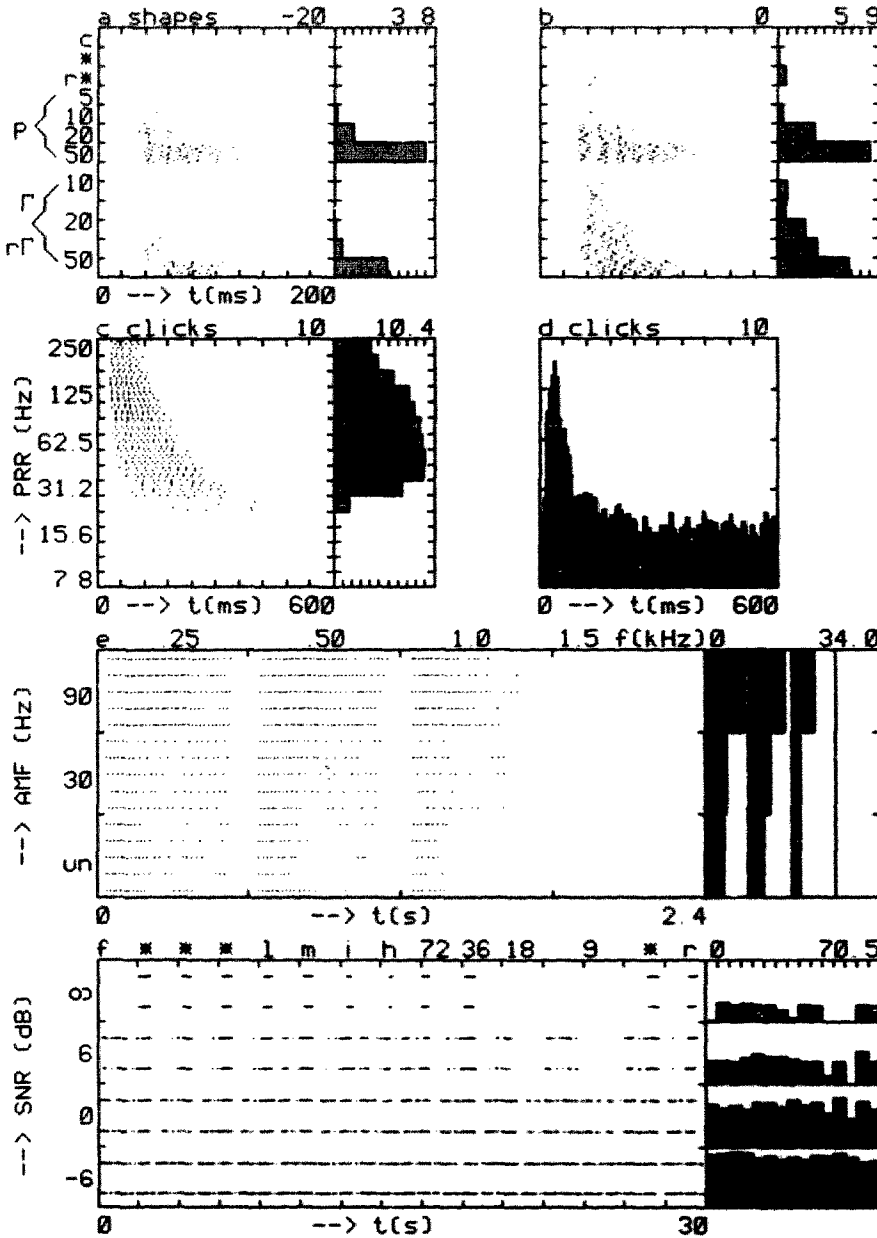


Fig. 6. Reordered event displays together with rate histograms of the model TS neuron of Fig. 4 in response to the stimuli of Fig. 5. Fig. 6c is equal to Figs. 4d-e. All stimuli were presented at the relative intensities of Fig. 5.

noise (SNR ∞) both unit 322,3,0 and the model neuron do not respond to the 9 and 18 Hz PRR variation, which implies a high-pass response with respect to PRR. In comparison with Fig. 5f the model neuron is less frequency selective: it responds weakly to the carrier frequency variations of 1067 and 1542 Hz (i and h). Unit 322,3,0

adapts to the noise, which is visible in the first 10 s of Fig. 5f. Thereafter, the response to the mating calls remains distinct up to the highest noise level. In contrast the model neuron's response to the calls is masked by the response to the noise for the highest two noise levels.

Now the same model is applied to a unit which

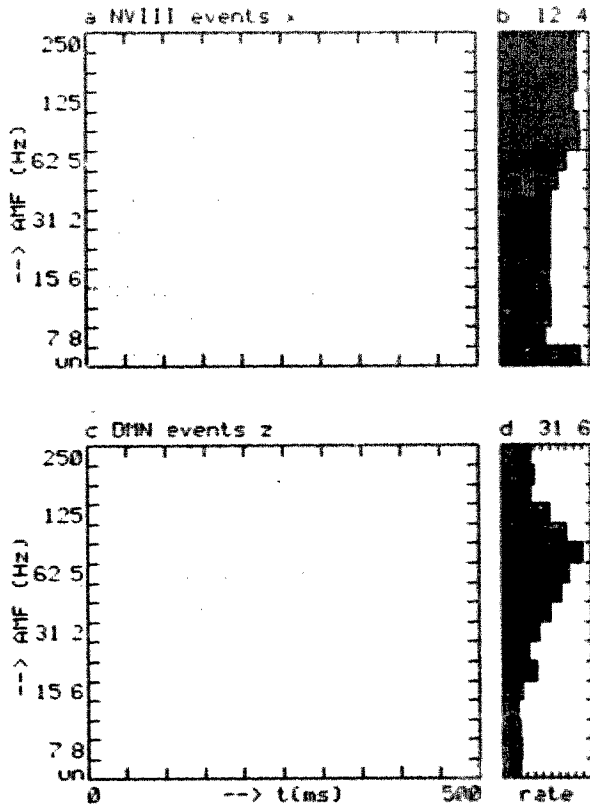


Fig. 7. Reordered event displays together with rate histograms of responses of first and second order model neurons to AM tonebursts. Stimulus parameters: intensity: 12 dB relative to r^0 , carrier frequency 0.55 kHz. Model parameters: tuning: centre frequency 0.625 kHz. All other parameters as in Fig. 5 except: EPSP shape: τ_d 1 ms; second order event generation: m 0.38.

did not respond to the pulse shape stimulus and which showed a band-pass response to both the click trains and the AM tone bursts. To model a band-pass response to the AM tone bursts the degree of coincidence detection on the DMN level is increased by shortening the EPSP and slightly increasing the thresholds. The effect of this is pictured in Fig. 7. The rate response of the NVIII unit shows a non-selective character (Fig. 7b). Note that the responses to the five presentations of each AM tone burst are aligned very well for AMFs around 62.5 Hz (Fig. 7a). Recall that the absolute refractory periods of the NVIII inputs varied between 3 and 6 ms, and their thresholds varied between 0.001 and 0.0001. Together with the relative refractory mechanism these dif-

ferences limit the ability of the NVIII inputs to respond simultaneously with the lowest and highest AMFs. This results in a DMN generator potential peak histogram with a band-pass character (not shown here, see Fig. 8 in Van Stokkum and Gelsen, 1989). Because of its high threshold the DMN unit produces a band-pass response with respect to AMF (Figs. 7c, d). Temporal integration of the four DMN inputs produces the generator potential characteristics of Figs. 8a-c. Both the averaged area and the averaged peak (Figs. 8b and c) show a band-pass character. The probability of event generation (Fig. 8f) utilizes this by means of a high threshold and produces a distinct band-pass response (Figs. 8d and e).

Now the response of unit 314,1,0 to six stimuli (Fig. 9) is compared with a model simulation (Fig. 10). Unit 314,1,0 did not respond to unmodulated tone bursts (Fig. 9e). Like unit 322,3,0 it received

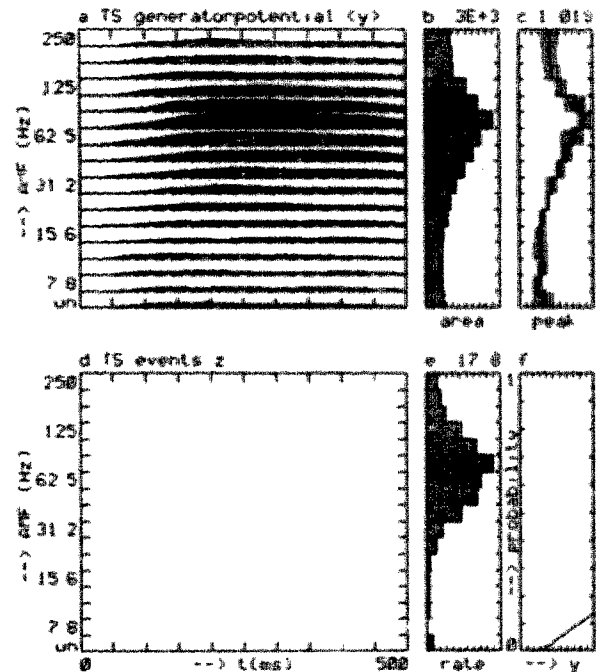


Fig. 8. Simulation of a TS neuron, which receives input from four DMN neurons as in Figs. 7c, d. Output: y , the generator potential, and z , the events, as a function of AMF. Inputs are four units, with m varying linearly between 0.35 and 0.38. The m -value of 0.38 was used in Figs. 7c, d. Model parameters for the third order neuron: EPSP shape: τ_d 100 ms, τ_r 70 ms. Parameters for the TS event generation: ν 1 (ms) $^{-1}$, m 0.3. A delay of 2 ms was incorporated. Refractory parameters: τ_{on} 15 ms, R 0.5, τ_R 5 ms.

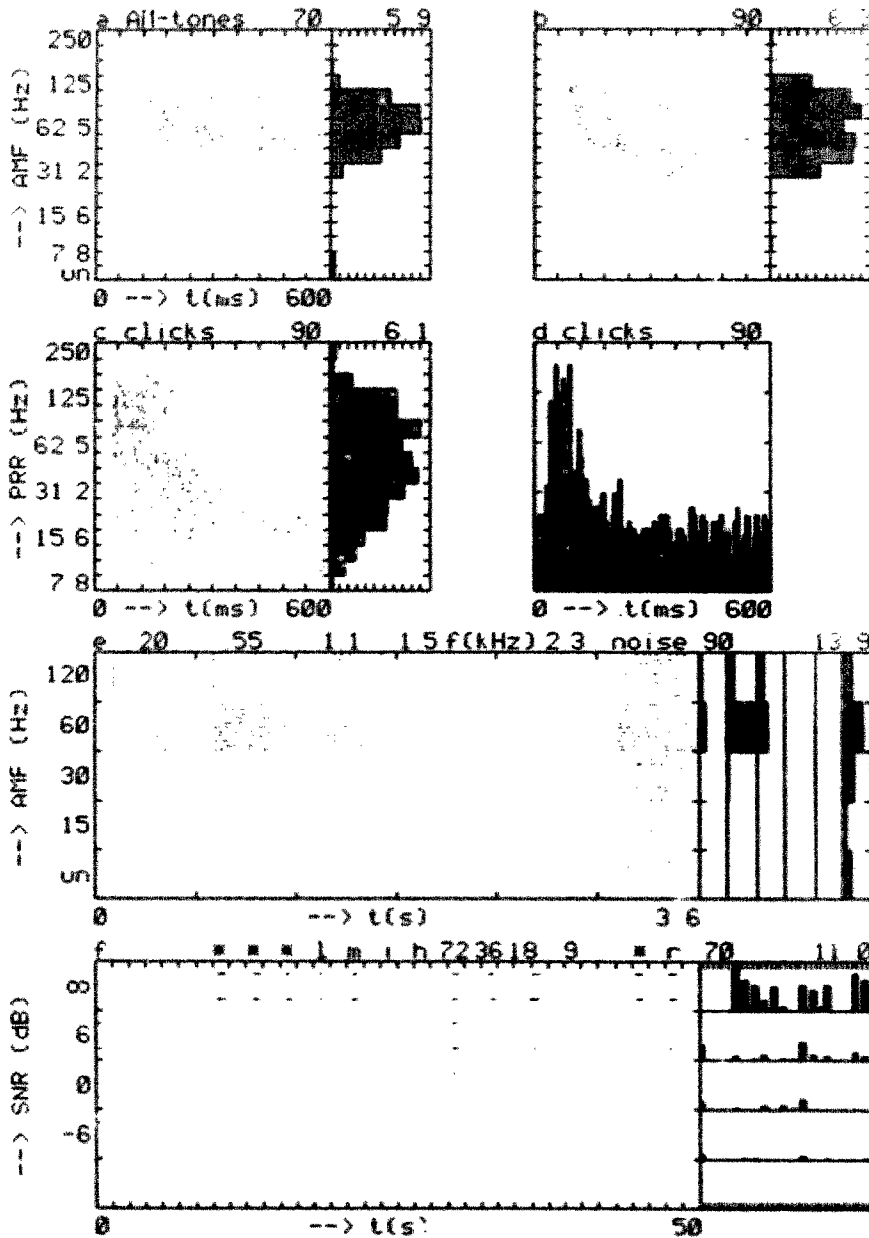


Fig. 9. Reordered event displays together with rate histogram of responses of TS unit 314.1.0 to six different stimuli. The AMF of the tonebursts (Figs. a and b) varied between 7.8 and 250 Hz, in addition an unmodulated toneburst (un) was presented. Carrier frequency in Figs. a and b was 0.55 kHz. With the spectrotemporal stimulus (Fig. c) carrier frequency varies horizontally between 0.2 and 2.3 kHz. In addition a white noise burst was used as carrier. AMF varies vertically between 15 and 120 Hz, in addition an unmodulated sound burst was presented. Rest of legend as in Fig. 5.

excitatory input derived from the amphibian papilla, which can be concluded from the response to carrier frequencies below 1.1 kHz in Fig. 9e. Its threshold was 50 dB peak SPL. The frequency selectivity is modelled with a band-pass filter tuned

to 0.625 kHz. In contrast to the band-pass response with AM tonebursts, the response to AM noise bursts (rightmost carrier) shows a weaker selectivity (Fig. 9e). This is reproduced well by the model (Fig. 10e). A more detailed investigation of

the AMF selectivity, using a carrier frequency of 0.55 kHz, is shown in Figs. 9a, b and 10a, b. At intensities differing by 20 dB a clear selectivity for AMFs between 31 and 125 Hz is visible. Note that the rate response to the AM tone burst with a carrier frequency of 0.55 kHz and an AMF of 60 Hz (Fig. 9e) is twice as large as the maximum

response in Fig. 9b. This points to a habituation effect caused by the repeated presentation of 0.55 kHz AM tone bursts, despite the onset interval of 3 s. At the highest intensity the model's response deviates in that the AMF selectivity is no longer absolute, some response is visible to the lower and higher AMFs. The response to the click trains in

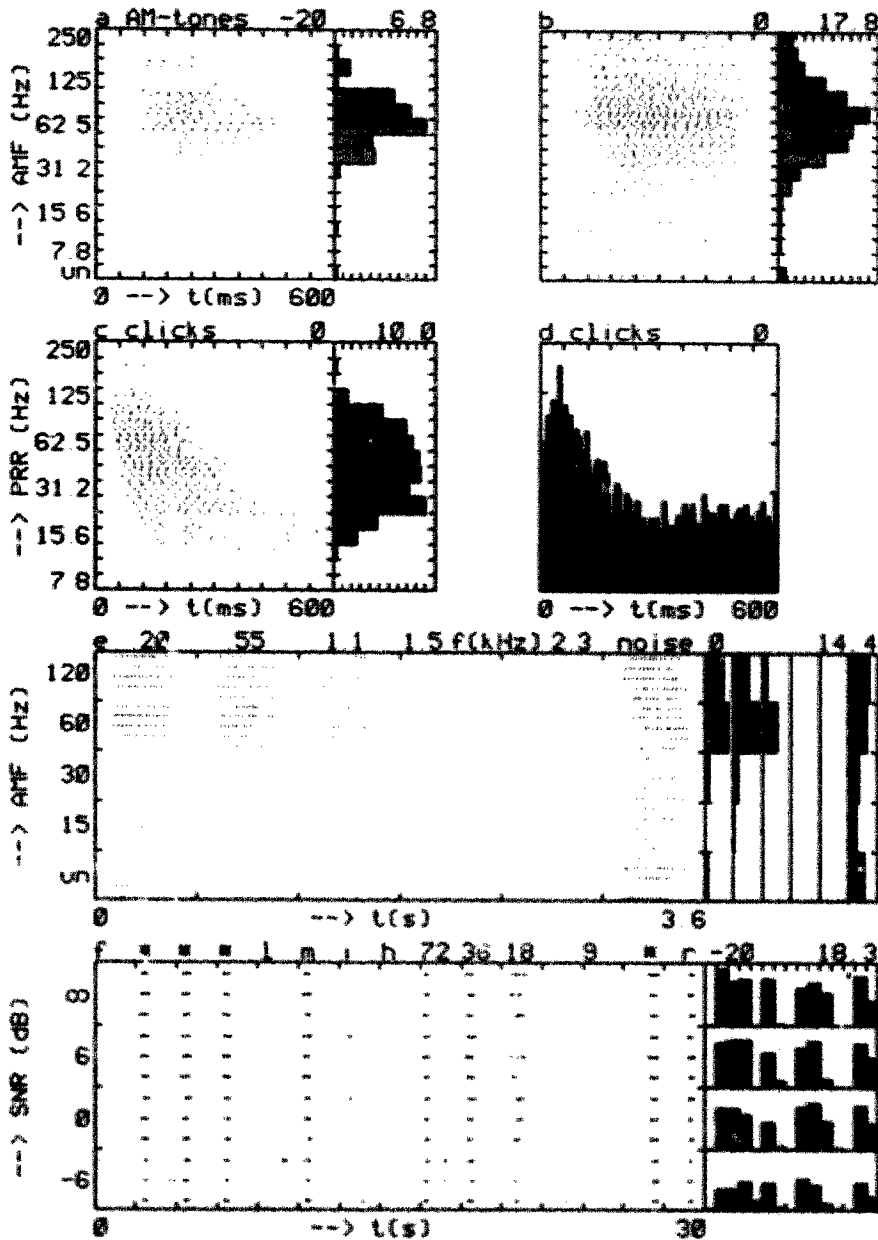


Fig. 10. Reordered event displays together with rate histogram of the model TS neuron of Fig. 8 in response to the stimuli of Fig. 9. Fig. 10b is equal to Figs. 8d-e. All stimuli are presented at the relative intensities of Fig. 9.

both cases shows a band-pass character (Figs. 9c and 10c). Unit 314,1,0 adapted totally after 90 s of the random click stimulus, which the model neuron did not (not shown). The crosscoincidence histograms (Figs. 9d and 10d) both show a broad peak, which is somewhat broader for the model neuron. Finally the responses to the mating call ensemble (Figs. 9f and 10f) agree with respect to the PRR variations in that no response is visible to the 9 Hz PRR variation. The frequency selectivity of the model agreed well at 90 dB peak SPL (compare Figs. 9e and 10e), but differed for the mating calls at 70 dB peak SPL, where unit 314,1,0 responded weakly to the carrier frequency variation of 201 Hz (I). Both unit 314,1,0 and the model neuron practically do not respond to the noise, which is visible in the first second of the reordered eventdisplays. The response of unit 314,1,0 is completely masked by the noise, except for the 72 Hz PRR variation. In contrast the response of the model neuron persists up to the highest noise level, which reminds us of the response of unit 322,3,0 in Fig. 5f.

Thus, from Figs. 3 to 10 it is concluded that a change of only a few parameters, notably the EPSP shapes between first and second, and between second and third order neurons, in concordance with the adjustment of the pulse generating properties, produces two model neurons which reflect most of the properties of two qualitatively different auditory midbrain units.

Discussion

Modelling

The model of the anuran auditory periphery (Van Stokkum and Gielen, 1989) has been extended to model the monaural properties of auditory midbrain neurons. Using a single parameter set the response of the model to a set of spectrally and temporally structured stimuli corresponded with the response characteristics of two typical TS neurons. Variation of only a few parameters, notably the EPSP shapes, produced characteristics corresponding with those of another TS neuron whose responses were qualitatively different. Together with the results of the previous paper it is concluded that variation of the parameters of this

monaural model reproduces most of the response characteristics found with NVIII fibres, DMN neurons and TS neurons without inhibition (see the discussion below).

Mechanisms

The different model stages, which correspond with different stations along the auditory pathway, perform different operations on the stimulus envelope. To begin with, in the NVIII a variety of short-term adaptation patterns exists (Megela and Capranica, 1981). In the DMN a group of units is selective for fast intensity changes, like the onsets of the mating call pulses (Hall and Feng, 1988; Van Stokkum, 1987). This was modelled with a coincidence detection mechanism, which detected synchrony of converging fast adapting NVIII inputs. In the TS a group of units possesses long integration times, which enables them to develop selectivity for pulse duration and PRR (this study). Using tonepips Bibikov (1977) found that 45% of the TS neurons have integration times in the range between 10 and 100 ms. This sample of 45% corresponds well with column two of Table II, which comprises the group of TS neurons that showed an integration effect with the pulse shape stimulus. Adding to this group the neurons which do not respond to pure tones (columns three of table II, unit 314,1,0) it is found that over half of the TS units possess integration times larger than 10 ms.

Examining the neuronal morphology of the TS, Feng (1983) observed a variety of soma shapes and dendritic lengths ranging from less than 100 μm to over 350 μm . Inputs arriving at large dendrites give rise to a long duration EPSP at the event generation site of the neuron (Rall, 1977). Intracellular recordings from neurons in the optic tectum of the grassfrog (Matsumoto et al., 1986) have shown that EPSP time constants of more than 10 ms are present. All this evidence supports the hypothesis that temporal integration is responsible for the temporal selectivities that appear for the first time in the TS. Differences in neuronal morphology may provide the different integrative properties. Next to the adaptation and spatiotemporal integration of inputs the event generation is crucial. A nonlinearity, the threshold

mechanism of Eq. 11, was necessary to produce the temporal selectivities on the DMN and TS level.

Parameter variation

The significance of the parameters of Table I will be discussed in connection with the various responses in Table II. A first group of parameters (γ , ω_1 , β_1 , ω_2 , r^0 , λ , μ , ω_2) is responsible for the NVIII generator potential w . Variation of ω_1 and β_1 produces different spectral selectivities. Variation of the adaptation parameters λ and μ produces the different types of short-term adaptation found in the NVIII by Megela and Capranica (1981). The neuronal refractory (τ_{abs} , R , τ_R) and event generation (ν , m) properties have to be adjusted to produce realistic response properties. Thereby τ_{abs} was chosen equal to the neuron's smallest interspike interval. The threshold m was responsible for the response selectivity derived from the generator potential.

Different firing patterns of NVIII inputs are a prerequisite for coincidence detection on the DMN level. These differences are caused by differences in threshold m and in absolute refractory period τ_{abs} , and by the relative refractory mechanism (R , τ_R). The second prerequisite for the coincidence detection is spatiotemporal integration. At least two inputs are necessary. The effect of reducing the decay time τ_d from 3 to 1 ms was demonstrated in this paper (Fig. 7, compare Figs. 6 and 10).

The larger τ_d and τ_u of the third order neuron, the more temporal integration. A neuron with small τ_d and τ_u will show a non-selective or low-pass response pattern with respect to PRR (rows 1 and 2 of Table II). These responses will be comparable to those shown in Figs. 3c, d. It was shown in Figs. 3-6 that the combination of moderate coincidence detection on the DMN level ($\tau_d = 3$ ms) with temporal integration on the TS level produced a high-pass response with respect to PRR (row 3 in Table II). Increase of the coincidence detection on the DMN level ($\tau_d = 1$ ms) in combination with temporal integration produced a band-pass response with respect to PRR (row 4 in Table II, Figs. 7-10). The majority of the units with a bimodal or no response to the

click trains showed signs of inhibition (see the discussion below).

Adaptation

Next to the adaptation in the NVIII it was assumed that there is also adaptation in the higher order neurons of the model. To model this a negative feedback was supplied to the DMN neuron, with a time constant of 400 ms. This improved the correspondence between data and model simulations. Because of methodological problems the recovery time constant μ was limited to 1000 ms. Non-stationarities involving longer time constants were found with the complete adaptation of unit 314,1,0 to the random click stimulus in 90 s and the adaptation to the noise of unit 322,3,0 in the first 10 s of Fig. 5f. These non-stationarities may be related to long-term adaptation or to habituation. Megela and Capranica (1983) found that NVIII fibres do not habituate to repeated stimuli, whereas in the TS habituation was observed with stimulus repetition rates larger than one per second. Presumably habituation is related to inhibitory processes, which were not included in the model.

Neural interaction

Epping and Eggermont (1987) investigated neural interaction in the grassfrog's TS. In a sample of 264 unit pairs they found that 60% of the pairs showed neural synchrony, which in 77% of the cases was caused by stimulus influences. The remaining 23% showed signs of two sorts of neural interaction: excitation (4%) and common input (19%). In the smaller sample of this paper 90% of the unit pairs showed neural synchrony, which in 83% of the cases was caused by the stimulus. This confirms the suggestion of Epping and Eggermont that their 60% neural synchrony was a lowerbound, because part of the unit pairs had not been tested with the more effective temporally structured stimuli.

There are two major shortcomings of the cross-correlation method. First, when spontaneous activity is low, as is the case in the TS, inhibition is almost undetectable (Melssen and Epping, 1987). Second, non-spiking interneurons, which have been

revealed in the grassfrog's optic tectum by Matsumoto et al. (1986), remain undetected. In view of the lack of information about inhibitory processes and non-spiking interneurons, no conclusion can be drawn about the importance of local circuits in the TS for the processing of temporal characteristics of sound.

Inhibition

In this paper inhibition was not included in the model. Inhibition has been demonstrated in the temporal domain by Bibikov (1981) who used random clicks and described a group of units receiving inhibitory input followed by excitatory input (type III of Epping and Eggermont, 1986a).

In the spectral domain Fuzessery and Feng (1982) demonstrated abundant two-tone inhibition. A neuron with high best-frequency which was inhibited by low and mid frequencies was simulated by extending the model with an inhibitory branch which started with a band-pass filter tuned to the best inhibitory frequency. This model neuron showed two-tone inhibition.

A problem with modelling inhibition is to derive the temporal properties of the inhibitory branch. Experiments using temporally structured two-tone stimuli are necessary to enable more systematic modelling.

Temperature dependence

Brenowitz et al. (1985) and Rose et al. (1985) have shown that the AMF selectivity of auditory midbrain units is temperature dependent. For one unit they found that the preferred AMF shifted from 15 to 25 Hz when the temperature was increased by 8°C. The model offers an explanation for this when the temperature dependence of the EPSP is taken into account. It is known that the Q_{10} of the membrane conductance (passive) is about 1.3 (Jack et al., 1983; p. 231; Mrose and Chiu, 1979). Thus a higher temperature will increase the membrane conductance and shorten the EPSP. A shorter EPSP between NVIII and DMN increases the preference for fast intensity changes, which are found with higher AMFs. A shorter EPSP between DMN and TS leads to less temporal integration, and causes a preference for

stimuli with a shorter periodicity, corresponding with higher PRRs and AMFs.

Identification and localization

So far only the processing of monaural stimuli was considered. Experiments using temporally structured binaural stimuli (Melssen and Van Stokkum, 1988) suggested that identification and localization of sound are coupled processes which make use of common mechanisms. So it would be worthwhile to extend the model to binaural stimuli in order to achieve a more complete picture of the information processing in the anuran auditory brain stem.

Acknowledgements

This investigation was supported by the Netherlands Organization for Scientific Research (NWO). Koos Braks skilfully prepared the animals. The experiments were conducted in close cooperation with Willem Melssen, who is also thanked for software assistance. Nikolai Bibikov, Willem Epping, Stan Gielen, Peter Johannesma, Willem Melssen, Henk van den Boogaard and two anonymous reviewers are thanked for helpful discussions and critical reading of the text.

References

- Aertsen, A.M.H.J. and Johannesma, P.I.M. (1980) Spectro-temporal receptive fields of auditory neurons in the grassfrog. I. Characterization of tonal and natural stimuli. *Biol. Cybern.* 38, 223–234.
- Aertsen, A.M.H.J., Vlaming, M.S.M.G., Eggermont, J.J. and Johannesma, P.I.M. (1986) Directional hearing in the grassfrog (*Rana temporaria* L.): II. Acoustics and modelling of the auditory periphery. *Hear. Res.* 21, 17–40.
- Bibikov, N.G. (1971a) The reaction of single neurons in the auditory system of the frog *Rana ridibunda* to pulsed tonal stimuli. *J. Evol. Biochem. Physiol.* 7, 178–185.
- Bibikov, N.G. (1971b) Responses of auditory neurons in the midbrain of the frog. *Proc. VIIth Int. Congr. Acoust., Budapest*, pp. 549–552.
- Bibikov, N.G. (1974) Encoding the stimulus envelope in peripheral and central regions of the acoustic system of the frog. *Acustica* 31, 301–305.
- Bibikov, N.G. (1975) Evaluation of the dynamics of synaptic potentials from the evoked impulse activity of the neurones. *Biophysics* 20, 901–906.

- Bibikov, N.G. (1977) The classification of the neurons in the auditory system on the basis of the function of the expected rate probability. *Akust. Zh.* 23, 346–355.
- Bibikov, N.G. (1978) Dynamics of the expected rate probability in auditory system neurons for different intensities of tonal stimuli. *Akust. Zh.* 24, 816–825.
- Bibikov, N.G. (1980) The reaction of the torus semicircularis units of *Rana temporaria* to the signals simulating the mating call temporal characteristics. *Zool. Zh.* 59, 577–586.
- Bibikov, N.G. (1981) Cross-correlation analysis of the activity of the auditory neurones on exposure to sound clicks. *Biophysics* 26, 346–352.
- Bibikov, N.G. and Kalinkina, T.V. (1983) Properties of the acoustic neurons of the dorsal medullary nucleus in *Rana ridibunda*. *J. Evol. Biochem. Physiol.* 18, 346–352.
- Bibikov, N.G. and Ivanitskii, G.A. (1985) Modelling spontaneous pulsation and short-term adaptation in the fibres of the auditory nerve. *Biophysics* 30, 152–156.
- Brenowitz, E.A., Rose, G. and Capranica, R.R. (1985) Neural correlates of temperature coupling in vocal communication system of the gray treefrog (*Hyla versicolor*). *Brain Res.* 359, 364–367.
- Brzoska, J. (1984) The electrodermal response and other behavioural responses of the grass frog to natural and synthetic calls. *Zool. Jb. Physiol.* 88, 179–192.
- Brzoska, J., Walkowiak, W. and Schneider, H. (1977) Acoustic communication in the grass frog (*Rana t. temporaria* L.): calls, auditory thresholds and behavioural responses. *J. Comp. Physiol.* 118, 173–186.
- Cox, D.R. and Isham, V. (1980) Point processes. Chapman and Hall, London.
- Crawford, A.C. and Fettilplace, R. (1980) The frequency selectivity of auditory nerve fibres and hair cells in the cochlea of the turtle. *J. Physiol.* 306, 79–125.
- Crawford, A.C. and Fettilplace, R. (1981) Non-linearities in the responses of turtle hair cells. *J. Physiol.* 315, 317–338.
- Dunia, R. and Narins, P.M. (1989) Temporal resolution in frog auditory-nerve fibers. *J. Acoust. Soc. Am.* 85, 1630–1638.
- Eggermont, J.J. (1985) Peripheral auditory adaptation and fatigue: A model oriented review. *Hear. Res.* 18, 57–71.
- Eggermont, J.J. and Epping, W.J.M. (1986) Sensitivity of neurons in the auditory midbrain of the grassfrog to temporal characteristics of sound. III. Stimulation with natural and synthetic mating calls. *Hear. Res.* 24, 255–268.
- Eggermont, J.J. and Epping, W.J.M. (1987) Coincidence detection in auditory neurons: A possible mechanism to enhance stimulus specificity in the grassfrog. *Hear. Res.* 30, 219–230.
- Epping, W.J.M. and Eggermont, J.J. (1985) Single unit characteristics in the auditory midbrain of the immobilized grassfrog. *Hear. Res.* 18, 223–243.
- Epping, W.J.M. and Eggermont, J.J. (1986a) Sensitivity of neurons in the auditory midbrain of the grassfrog to temporal characteristics of sound. I. Stimulation with acoustic clicks. *Hear. Res.* 24, 37–54.
- Epping, W.J.M. and Eggermont, J.J. (1986b) Sensitivity of neurons in the auditory midbrain of the grassfrog to temporal characteristics of sound. II. Stimulation with amplitude modulated sound. *Hear. Res.* 24, 55–72.
- Epping, W.J.M. and Eggermont, J.J. (1987) Coherent neural activity in the auditory midbrain of the grassfrog. *J. Neurophysiol.* 57, 1464–1483.
- Feng, A.S. (1983) Morphology of neurons in the torus semicircularis of the northern leopard frog, *Rana pipiens pipiens*. *J. Morphol.* 175, 253–269.
- Feng, A.S. (1986) Afferent and efferent innervation patterns of the cochlear nucleus (dorsal medullary nucleus) of the leopard frog. *Brain Res.* 367, 183–191.
- Fritzsche, B., Ryan, M.J., Wilczynski, W., Hetherington, T.E. and Walkowiak, W. (Eds.) (1988) *The Evolution of the Amphibian Auditory System*. Wiley, New York.
- Fuzessery, Z.M. and Feng, A.S. (1982) Frequency selectivity in the anuran auditory midbrain: Single unit responses to single and multiple tone stimulation. *J. Comp. Physiol.* 146, 471–484.
- Fuzessery, Z.M. and Feng, A.S. (1983) Frequency selectivity in the anuran medulla: excitatory and inhibitory tuning properties of single neurons in the dorsal medullary and superior olivary nuclei. *J. Comp. Physiol.* 150, 107–119.
- Hall, J.C. and Feng, A.S. (1988) Influence of envelope rise time on neural responses in the auditory system of anurans. *Hear. Res.* 36, 261–276.
- Jack, J.J.B., Noble, D. and Tsien, R.W. (1983) *Electric current flow in excitable cells*. Clarendon Press, Oxford.
- Johannesma, P.I.M. (1971) Dynamical aspects of the transmission of stochastic neural signals. In: E. Broda, A. Locker, H. Springer-Lederer (Eds.), *First European Biophysics Congress*, Verlag der Wiener Medizinischen Akademie, Vienna, pp. 329–333.
- Johannesma, P.I.M. and Van den Bogaard, H.F.P. (1985) Stochastic formulation of neural interaction. *Acta Applic. Math.* 4, 201–224.
- Matsumoto, N., Schwippert, W.W. and Ewert, J.-P. (1986) Intracellular activity of morphologically identified neurons of the grass frog's optic tectum in response to moving configurational stimuli. *J. Comp. Neurophysiol.* A 159, 721–739.
- Megela, A.L. and Capranica, R.R. (1981) Response patterns to tone bursts in peripheral auditory system of anurans. *J. Neurophysiol.* 46, 465–478.
- Megela, A.L. and Capranica, R.R. (1983) A neural and behavioural study of auditory habituation in the bullfrog, *Rana catesbeiana*. *J. Comp. Physiol.* 151, 423–434.
- Melssen, W.J. and Epping, W.J.M. (1987) Detection and estimation of neural connectivity based on crosscorrelation analysis. *Biol. Cybern.* 57, 403–414.
- Melssen, W.J. and Van Stokkum, I.H.M. (1988) Selectivity for interaural time-difference and amplitude-modulation frequency in the auditory midbrain of the grassfrog. In: H. Duifhuis, J.W. Horst and H.P. Wit (Eds.) *Basic Issues in Hearing*, Academic Press, London, pp. 279–284.
- Mrose, H.E. and Chiu, S.Y. (1979) Is the steady state inactivation curve for the sodium channel temperature dependent? *Biophys. J.* 25, 193a.
- Perkel, D.H., Gerstein, G.L. and Moore, G.P. (1967) Neuronal spike trains and stochastic point processes. II. Simultaneous spike trains. *Biophys. J.* 7, 419–440.

- Potter, H.D. (1965) Patterns of acoustically evoked discharges of neurons in the mesencephalon of the bullfrog. *J. Neurophysiol.* 28, 1155–1184.
- Rall, W. (1977) Core conductor theory and cable properties of neurones. In: *Handbook of Physiology, Sect. 1: The nervous system Vol. I: Cellular biology of neurons, Part 1*, American Physiological Society, Bethesda MD, pp. 39–97.
- Rose, G.J. and Capranica, R.R. (1983) Temporal selectivity in the central auditory system of the leopard frog. *Science* 219, 1087–1089.
- Rose, G.J. and Capranica, R.R. (1984) Processing amplitude-modulated sounds by the auditory midbrain of two species of toads: matched temporal filters. *J. Comp. Physiol. A* 154, 211–219.
- Rose, G.J. and Capranica, R.R. (1985) Sensitivity to amplitude modulated sounds in the anuran auditory nervous system. *J. Neurophysiol.* 53, 446–465.
- Rose, G.J., Brenowitz, E.A. and Capranica, R.R. (1985) Species specificity and temperature dependency of temporal processing by the auditory midbrain of two species of treefrogs. *J. Comp. Physiol. A* 157, 763–769.
- Schneider-Lowitz, B. (1983) Neuronaler Verarbeitung einfacher und komplexer Schallsignale in der Peripherie und den unteren Stationen der Hörbahn des Grassfrosches (*Rana t. temporaria* L.). Thesis, Bonn, F.R.G.
- Van den Boogaard, H.F.P. (1988) System identification based on point processes and correlation densities. II. The refractory neuron model. *Math. Biosci.* 91, 35–65.
- Van Gelder, J.J., Evers, P.M.G. and Maagnus, G.J.M. (1978) Calling and associated behaviour of the common frog, *Rana temporaria*, during breeding activity. *J. Anim. Ecol.* 47, 667–676.
- Van Stokkum, I.H.M. (1987) Sensitivity of neurons in the dorsal medullary nucleus of the grassfrog to spectral and temporal characteristics of sound. *Hear. Res.* 29, 223–235.
- Van Stokkum, I.H.M. (1989) Analysis of auditory brainstem neurons in the grassfrog. Thesis, Univ. of Nijmegen.
- Van Stokkum, I.H.M. and Gielen, C.C.A.M. (1989) A model for the peripheral auditory system of the grassfrog. *Hear. Res.* 41, 71–86.
- Vlaming, M.S.M.G., Aertsen, A.M.H.J. and Epping, W.J.M. (1984) Directional hearing in the grassfrog (*Rana temporaria* L.): I. Mechanical vibrations of the tympanic membrane. *Hear. Res.* 14, 191–201.
- Walkowiak, W. (1984) Neuronal correlates to the recognition of pulsed sound signals in the grass frog. *J. Comp. Physiol. A* 155, 57–66.
- Walkowiak, W. (1988) Central temporal encoding. In: B. Fritsch et al. (Eds.), *The Evolution of the Amphibian Auditory System*, Wiley, New York, pp. 275–294.
- Walkowiak, W. and Brzoska, J. (1982) Significance of spectral and temporal call parameters in the auditory communication of male grass frogs. *Behav. Ecol. Sociobiol.* 11, 247–252.
- Wilczynski, W. (1988) Brainstem auditory pathways in anuran amphibians. In: B. Fritsch et al. (Eds.), *The Evolution of the Amphibian Auditory System*, Wiley, New York, pp. 209–231.
- Zakon, H.H. and Wilczynski, W. (1988) The physiology of the anuran eighth nerve. In: B. Fritsch et al. (Eds.), *The Evolution of the Amphibian Auditory System*, Wiley, New York, pp. 125–155.